

SPECIFIC FEATURES OF ${}^6\text{He}$ IN NUCLEAR REACTIONS INDUCED BY α -PARTICLES*

B.A. URAZBEKOV, D.M. JANSEITOV

Institute of Nuclear Physics, 1 Ibragimov St, Almaty 050032, Kazakhstan
and
BLTP, JINR, 20 Joiliot Curie St, Dubna 141980, Russia

A.S. DENIKIN

Dubna State University, 19 Universitetskaya St, Dubna 141982, Russia
and
FLNR, JINR, 20 Joiliot Curie St, Dubna 141980, Russia

(Received November 9, 2021; accepted November 9, 2021)

A three-body model $\alpha + 2N$ for ${}^6\text{He}$ is applied using the wave function obtained within the stochastic variational method based on the Gaussian basis. An explicit expression is obtained for the density distribution function of nuclear matter. The elastic scattering of ${}^6\text{He}$ by α -particles is studied in detail. By employing the calculated density distribution functions, the folding interaction potentials are built. The resulting folding potential is applied to calculate the differential cross sections of elastic scattering in the framework of the optical model. In order to treat the excess experimental cross sections at the large angles, the mechanisms of two nucleon transfer are proposed. With the proposed theoretical approach, good agreement in the comparison of calculated differential cross sections with the experimental data is demonstrated. It is also shown that the two-step transfer mechanisms of two nucleons predominate over one-step transfer mechanisms.

DOI:10.5506/APhysPolBSupp.14.799

1. Introduction

In the light nuclei, the cluster structure can often clearly manifest itself in the dripline region of the nuclear map. These series include such nuclei as ${}^6\text{He}$, ${}^{11}\text{Li}$, ${}^{12}\text{Be}$, and other exotic nuclei. However, there are also stable

* Presented at III International Scientific Forum “Nuclear Science and Technologies”, Almaty, Kazakhstan, September 20–24, 2021.

nuclei with apparent cluster structures. These include such nuclei as ${}^6\text{Li}$, ${}^9\text{Be}$, ${}^{11}\text{B}$, and others. Numerous experimental data [1–3] allow us to treat such nuclei as multi-cluster systems, including tightly bound α -clusters and valence nucleons. For these nuclei, the relative motion of internal subsystems determines the property and mechanisms of nuclear reactions. The simplest nucleus with a cluster structure as ${}^6\text{He}$ is ideally suited for consideration within the framework of the three-body model. Moreover, it should be noted that the interaction of pairs inside these nuclei is well known, which can be used in constructing a solution to the Schrödinger equation. An important factor is also the number of scattering experiments conducted to study the structures of these nuclei.

There are many theoretical approaches [4–6] devoted to studying the structure of exotic nuclei. In particular, the nuclear excitation function for light exotic nuclei is well reproduced by the No Core Shell Model (NCSM) [7, 8]. The method uses a one-particle basis function of the harmonic oscillator, realistic NN , NNN interactions. This method is reduced to solving the A -nucleon Schrödinger equation on the basis containing all possible configurations of A -nucleon oscillator functions. However, the size of the basis grows rapidly with the number of nucleons, the reliability of the NCSM model calculations decreases in the case of heavy nuclei. At present, the capabilities of modern computational machines make it possible to perform calculations with sufficient accuracy for nuclei with masses $A \leq 16$.

The experimental data of elastic scattering of ${}^6\text{He} + \alpha$ is available at the laboratory energy of 151 MeV [9, 10]. These experimental data can be used to show the elastic transfer phenomenon through the two-neutron transfer between the two α -core. The main motivation of these studies was to probe the relative importance of the “di-neutron” and “cigar” configurations of the valence neutrons in the ${}^6\text{He}$ ground state. The data show the backward angle rise in the cross section. Usually, it is considered as an indication of characteristics of elastic transfer. The DWBA analysis using the ${}^6\text{He}$ wave function built on hyper-spherical harmonics [6] showed good agreement with the backward angle data. Consequently, it is concluded that the di-neutron configuration dominates the ${}^6\text{He}$ ground state wave function. More detailed study of $\alpha + {}^6\text{He}$ scattering data has been carried out in Ref. [11] in the framework of the Coupled Reaction Channels (CRC) method.

In the present work, the three-body model $\alpha + 2n$ and its role in the mechanisms of nuclear reactions is investigated. Mostly, the features of the intrinsic structure of colliding nuclei in the interaction potentials are neglected, and taken in a phenomenological way, like in Gaussian form, or in the form of the Woods–Saxon potential. In such cases, one could take the potential in a more realistic shape of colliding nuclei. To describe direct nuclear reactions, we proceed from the natural shape of colliding nuclei

within the three-body model. Therefore, the motivation for this work is to minimize the number of free parameters in the calculations of nuclear reactions as much as possible, and to use the density distribution functions of nuclear matter based on the three-body model.

2. Three-body wave function

Consider a three-body system containing k , p , and q particles. A total wave function of this system with total spin J and spin projection M can be represented as a sum of components

$$\Psi^{JM}(\mathbf{x}_k, \mathbf{y}_k) = \sum_{\gamma} \Psi_{\gamma}^{JM}(\mathbf{x}_k, \mathbf{y}_k). \tag{1}$$

The vector \mathbf{x}_k is for the relative distance between the pair of particles pq and k , and \mathbf{y}_k is the vector of the relative distance between the center of mass of the pair pq and the particle k (see Fig. 1). The designation γ is equivalent to the set of quantum numbers $\lambda l L S$. The momenta λ, l are the orbital momenta conjugated to the coordinates \mathbf{x}_k , and \mathbf{y}_k , respectively, L is the total orbital momentum of the system, and S is the total spin of the three-body system. The each component defines spatial and spin parts as follows:

$$\begin{aligned} \Psi_{\gamma}^{JM}(\mathbf{x}_k, \mathbf{y}_k) &= \left[\Phi_L^{(\lambda, l)}(\mathbf{x}_k, \mathbf{y}_k) \otimes \chi_S(k, pq) \right]_{JM} \\ &= \sum_{M_L M_S} (L M_L S M_S | J M) \Phi_{L M_L}^{(\lambda, l)}(\mathbf{x}_k, \mathbf{y}_k) \chi_{S M_S}(k, pq), \end{aligned} \tag{2}$$

where $\chi_{S M_S}$ is the spin function.

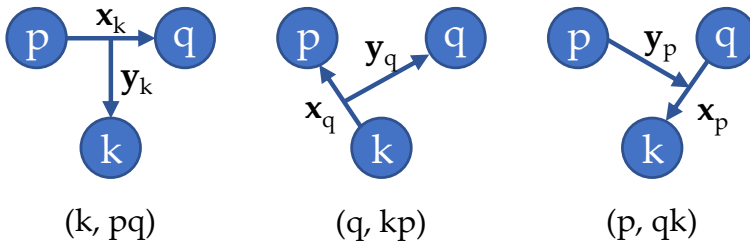


Fig. 1. The schemes of Jacobi coordinate sets for the three-body system.

The spatial part of the wave function is chosen to be multidimensional Gaussian functions of the form of

$$\begin{aligned} \Phi_{L M_L}^{(\lambda, l)}(\mathbf{x}_k, \mathbf{y}_k) &= x^{\lambda} y^l \sum_i C_i \exp \left(-\alpha_i^{(k)} x_k^2 - \beta_i^{(k)} y_k^2 \right) \\ &\quad \times [Y_{\lambda}(\hat{x}_k) \otimes Y_l(\hat{y}_k)]_{L M_L}. \end{aligned} \tag{3}$$

Here, the coefficients $\alpha_i^{(k)}$, $\beta_i^{(k)}$, and C_i are the parameters of the wave function expansion. In particular, C_i is found as a result of solving the generalized eigenvalue problem.

3. Density distribution functions

The density distribution function of nuclear matter within the three-body model can be expressed as follows:

$$\rho(\mathbf{R}) = \sum_{\iota=\{k,p,q\}} \rho^{(\iota)}(\mathbf{R}), \quad (4)$$

where $\iota = \{k, p, q\}$. The density function of a cluster is given by

$$\rho^{(\iota)}(\mathbf{R}) = \langle \Psi_{\text{tot}}^{JM} | \hat{\rho}_i | \Psi_{\text{tot}}^{JM} \rangle. \quad (5)$$

Here, the operator of density is defined as

$$\hat{\rho}_i \equiv \begin{cases} \delta(\mathbf{y}_i - y_0^{(i)} \mathbf{R}) & \text{for } i^{\text{th}} \text{ nucleons,} \\ \rho_\alpha(\mathbf{y}_i - y_0^{(i)} \mathbf{R}) & \text{for } i^{\text{th}} \alpha\text{-clusters,} \end{cases} \quad (6)$$

where $\delta(\mathbf{z})$ — delta function, $\rho_\alpha(\mathbf{r})$ — internal density distribution function of α -cluster

$$\rho_\alpha(\mathbf{r}) = \rho_0 \exp(-\gamma_0 \mathbf{r}^2). \quad (7)$$

The α -particle density function is normalized to unity with the following parameters:

$$\gamma_0 = \frac{3}{2} \frac{1}{\langle r_\alpha^2 \rangle}, \quad \rho_0 = \left(\frac{\gamma_0}{\pi} \right)^{\frac{3}{2}}. \quad (8)$$

Here, the square root of $\langle r_\alpha^2 \rangle$ — r.m.s. matter radius of α -particle, which equals 1.461 fm [12].

Provided the cluster k is α -particle, a relevant matrix element has the form of

$$\begin{aligned} & \langle \phi_{\gamma_i}^{JM}(k, pq) | \rho_\alpha(\mathbf{y}_k - y_0^{(k)} \mathbf{R}) | \phi_{\gamma'_j}^{JM}(k, pq) \rangle \\ &= \rho_0 C_i C_j \exp(-\gamma_0 R^2) \int \int dx_k dy_k x_k^2 y_k^2 \varphi_i^{(\lambda, l)}(x_k, y_k) \varphi_j^{(\lambda, l)}(x_k, y_k) \\ & \times \exp\left(-\gamma_0 y_0^{(k)2} y_k^2\right) i_0\left(2\gamma_0 y_0^{(k)} y_k R\right) \delta_{\gamma\gamma'}, \end{aligned} \quad (9)$$

where $i_l(x)$ is the modified spherical Bessel function of the first kind.

The density function of the α -particle k is built as follows:

$$\rho^{(\alpha k)}(R) = \sum_{\gamma} \rho_{\gamma}^{(\alpha k)}(R), \tag{10}$$

where

$$\begin{aligned} \rho_{\gamma}^{(\alpha k)}(R) &= 4\pi\rho_0 \exp(-\gamma_0 R^2) \sum_{ij} C_i C_j \mathcal{I} \left(2\lambda + 2, \frac{1}{2}\alpha_{ij}^{(k)} \right) \\ &\times \mathcal{I} \left(l, 0, \beta_{ij}^{(k)} + 2y_0^{(k)2} \gamma_0, 2\gamma_0 y_0^{(k)} R \right). \end{aligned} \tag{11}$$

Here, $\mathcal{I}(n, l, v, |w|)$ is given by (see [13], p. 270)

$$\mathcal{I}(n, l, v, |w|) = \frac{\pi (2n)!! |w|^l}{2 v^{n+l+3/2}} \exp\left(\frac{w^2}{2v}\right) L_n^{l+1/2}\left(-\frac{w^2}{2v}\right), \tag{12}$$

where, $L_n^{l+1/2}(x)$ is the associated Laguerre polynomial.

Let us turn to the density functions of q particles. In order to calculate the matrix elements for these particles, one must switch basis functions into (q, kp) Jacobi coordinate set. In particular, the matrix element for the nucleon q may be represented in the form of

$$\begin{aligned} &\langle \phi_{\gamma_i}^{JM}(k, pq) | \delta(\mathbf{y}_q - y_0^{(q)} \mathbf{R}) | \phi_{\gamma_j}^{JM}(k, pq) \rangle \\ &= \sum_{\tilde{\gamma}\tilde{\gamma}'} A_{\mathbf{Q}_j}^{\tilde{\lambda}\tilde{l}\tilde{\lambda}'\tilde{l}'} A_{\mathbf{Q}_i}^{\tilde{\lambda}\tilde{l}\tilde{\lambda}\tilde{l}} \langle \phi_{\tilde{\gamma}_i}^{JM}(q, kp) | \delta(\mathbf{y}_q - y_0^{(q)} \mathbf{R}) | \phi_{\tilde{\gamma}_j}^{JM}(q, kp) \rangle, \end{aligned} \tag{13}$$

where $A_{\mathbf{Q}_j}^{\tilde{\lambda}\tilde{l}\tilde{\lambda}'\tilde{l}'}$ is the transformation coefficient of the basis function (see details in Ref. [13]). The density function of the nucleon q may be represented as follows:

$$\rho^{(Nq)}(R) = \sum_{\gamma} \rho_{\gamma}^{(Nq)}(R), \tag{14}$$

where the component γ is

$$\rho_{\gamma}^{(Nq)} = \sum_{\tilde{\gamma}ij} A_{\mathbf{Q}_{ij}}^{\tilde{\lambda}\tilde{l}\tilde{\lambda}^2} C_i C_j \left(y_0^{(q)} \right)^{2\tilde{l}} R^{2\tilde{l}} \exp\left(-\frac{1}{2}y_0^{(q)2} \beta_{ij}^{(q)} R^2\right) \mathcal{I} \left(2\tilde{\lambda} + 2, \frac{1}{2}\alpha_{ij}'^{(q)} \right). \tag{15}$$

Here, the integral $\mathcal{I}(\lambda, \alpha)$ is given by

$$\mathcal{I}(\lambda, \alpha) = 2^{1+\lambda} \frac{\Gamma(1+\lambda)}{(\alpha)^{1+\lambda}}, \tag{16}$$

where $\Gamma(x)$ — the Gamma function.

Density functions for the nucleon N_p are obtained in a similar way as for density functions for the nucleon N_q .

4. Results and discussions

4.1. The density functions of nuclear matter

On the basis of the three-body wave function (1), the nuclear matter density distributions are calculated for ${}^6\text{He}$ in the ground state. The results are shown in Fig. 2. The plotted density functions are normalized to their own atomic masses.

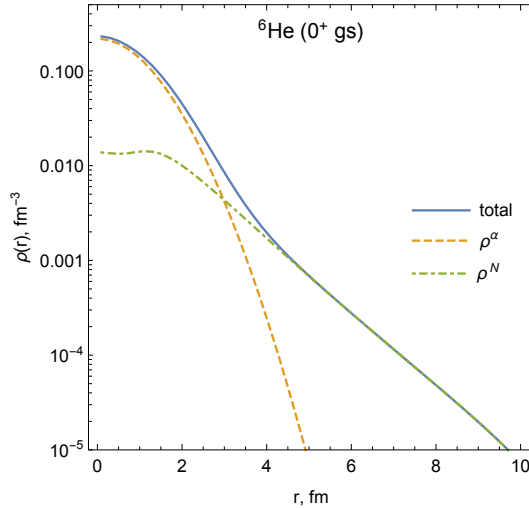


Fig. 2. The nuclear matter density distribution of ${}^6\text{He}$ with the cluster component contributions.

A distinctive feature of the obtained results is in the extended tail of the density function. This is caused by the properties of the valence nucleons in the three-body system. In particular, the density function of the core $\rho^\alpha(r)$ tends rapidly to zero as the radius r increases in comparison with the nucleon density function ρ^N . Another point of behaviour of the density function is a maximum in the density functions ρ^N at $r \simeq 1.8$ fm. This character of function explains that the valence nucleons are moved apart from the c.m.

A comparison of the total density function $\rho(r)$ for ${}^6\text{He}$ with the density function calculated in the framework of the Large-Scale Shell-Model (LSSM) (for more, see Ref. [14]) is illustrated in Fig. 3. Both functions are in good agreement. However, starting from $r \simeq 5.0$ – 10.0 fm, the three-body model is slightly overestimated.

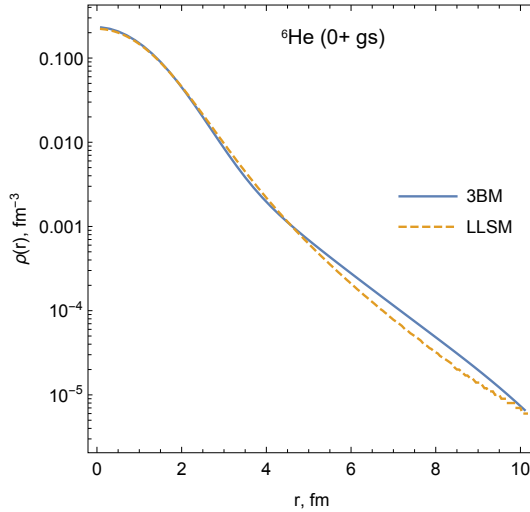


Fig. 3. The comparison of the total nuclear matter density distribution function within the three-body model (3BM) with the LSSM calculations (LSSM) [14] for ${}^6\text{He}$.

4.2. ${}^6\text{He} + \alpha$ reaction

The differential cross section of elastic scattering for the ${}^6\text{He} + \alpha$ nuclear reaction has been calculated within the framework of the OM. The calculations were carried out by means of the FRESKO code [15].

The optical potential for the ${}^6\text{He} + \alpha$ system was obtained within the DF model using the density functions of nuclear matter. For the NN -force the density-dependent DDM3Y-Paris potential was chosen [16]. The DF potential may have terms depending on the interaction of projectile with the clusters of the three-body system. In particular, for the ${}^6\text{He} + \alpha$ system, the DF potential can be defined as

$$V^{\text{DF}}(r) = V_{\alpha+\alpha}^{\text{DF}}(r) + V_{2N+\alpha}^{\text{DF}}(r). \quad (17)$$

The calculated results are demonstrated in Fig. 4. The folding potentials of α -core and two valence nucleons with the projectile ${}^4\text{He}$ show specific feature of the interaction. The potential of the α -cluster with the projectile provides a strong central part, while the interaction with halo neutrons is localized at the peripheral region.

The obtained potential was used to calculate the differential cross section for elastic scattering of ${}^6\text{He}$ by α -particles at the energy of $E_{\text{lab}} = 151$ MeV. As the real part of the optical potential, the folding potential with the parameter N_r was used. For the imaginary part of the optical potential, we

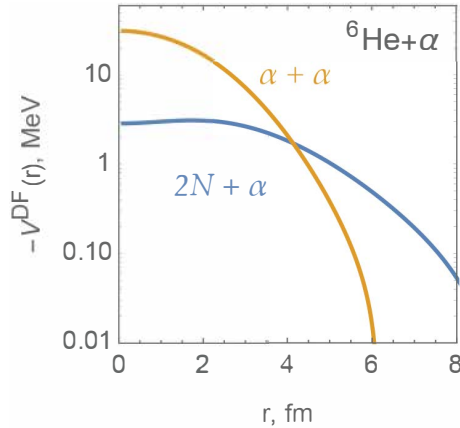


Fig. 4. The folding potential V^{DF} calculated by means of the density functions of ${}^6\text{He}$.

used again the folding potential, but with the parameter N_i . The corresponding results are shown in Fig. 5. The potential parameters used in the OM calculations are presented in Table I. The advantage of folding potential is in a less number of adjustable optical parameters. Instead of six parameters fitted in the case of Woods–Saxon potentials [10], the folding potential allows to reproduce data within two parameters.

TABLE I

Parameters of the double folding potential used in OM, and CRC calculations for the ${}^6\text{He} + \alpha$ nuclear reaction.

	N_r	N_i	χ^2/N
DF- ${}^6\text{He}$	$N_r = 1.4$	$N_i = 0.5$	7.32

Theoretical curves could show a good result in describing the experimental data on elastic scattering within the framework of the optical model. However, this is true only at the front scattering angles, while the backscattering angles are far from a description of optical calculations. Therefore, in order to explain the disagreement, we propose the following transfer mechanisms of two nucleons: the one-step and two-step transfer. Taking into account these mechanisms, the differential cross section can be written as follows:

$$\frac{d\sigma}{d\Omega}(\theta) = |f(\theta)_{\text{OM}}(\theta) + f_{\text{tr}}(\theta)|^2, \quad (18)$$

where $f(\theta)_{\text{OM}}$ is the scattering amplitude of elastic channel, f_{tr} — amplitude

of the transfer mechanisms, which approximately is

$$f_{\text{tr}}(\theta) \approx f_{\text{one}}(\pi - \theta) + f_{\text{two}}(\pi - \theta). \quad (19)$$

Here, f_{one} — an amplitude of finite-range transfer which may be calculated within the DWBA method, f_{two} — an amplitude of the two-step transfer mechanism (see, *i.e.* [15, 17]).

Obtained calculation results for the differential cross section of the elastic transfer were carried out within the framework of the CRC method [15]. Potential for the input and output channels was chosen to be the double folding potential ${}^6\text{He}$ -DF. The potential for the intermediate channel was taken as the optical potential with global optical parametrizations for α -particles [18]. Trial calculations have shown that the results depend insignificantly on the selected potential for the intermediate channel. The wave function of the bound states was chosen by fitting the potential depth to the binding energy of the composite systems. In particular, the binding energy of one neutron with ${}^6\text{He}$ was chosen to be 1.8 MeV, neutron with ${}^5\text{He}$ — 0.1 MeV, and two neutrons with α — 0.9 MeV.

The results of the CRC calculations for the elastic transfer are shown in Fig. 5. The elastic collision mechanism prevails at the forward scattering angles. Starting from the angle 90° , the contribution to the cross section

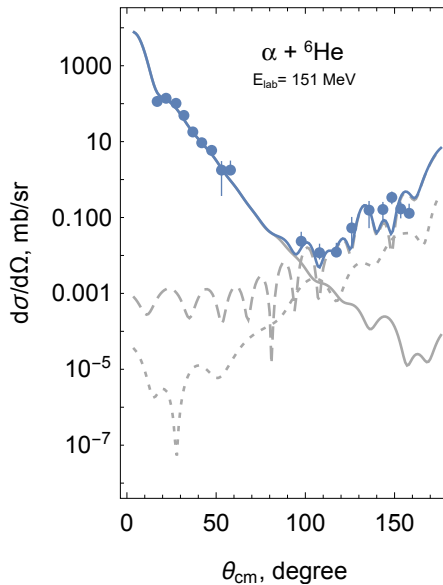


Fig. 5. (Colour on-line) The cross sections of the elastic channel with the few possible reaction mechanisms: elastic scattering (solid gray), one-step transfer of di-neutron (dashed gray), two-step transfer of di-neutron (dotted gray), and coherent sum (solid black/blue). Experimental data from [10].

is mainly caused by the two-step transfer mechanism. It is worth noting here that two neutrons have the $2S_0$ configuration, which, possibly, leads to an oscillatory cross section. One magnitude less is the contribution of the sequential transfer of di-neutron. In this case, both neutrons have $1P_{3/2}^2$ configuration. For the best reproduction of the experimental data, the SA of di-neutrons was taken as $\mathcal{A}_{2S_0}^{00} \approx 1.0$. The extracted value corresponds with the value from Refs. [10, 11].

Thus, it was possible to achieve good agreement between the calculated differential cross section, using the double-folding potential DF- ${}^6\text{He}$ and the proposed transfer mechanisms, with the experimental data [10].

5. Conclusion

In the framework of the double folding model, the interaction potential $\alpha + {}^6\text{He}$ has been calculated. It should be pointed out that the large diffuseness of the double folding potentials is caused by the valence nucleons. The potential built on the three-body density functions was used to calculate the differential cross sections of elastic, and nuclear transfer reactions.

The nuclear ${}^6\text{He} + \alpha$ reactions at the laboratory energy of 151 MeV are excellent tools in terms of the theoretical study. By using them, we could extract the optical potential parameters, the spectroscopic information of the three-cluster configurations. The spectroscopic amplitude of di-neutron in ${}^6\text{He}$ is consistent with the spectroscopic information given in Refs. [10, 11].

The experimental data on the elastic scattering of α -particles by ${}^6\text{He}$ demonstrate a significant growth of cross section at backward angles. This kind of behaviour is characterized by the contribution of the elastic transfer channel. The analysis based on the CRC calculations shows that the major contribution to the elastic transfer cross section is a result of the di-nucleon transfer channel. The two-step transfer is one order of magnitude lower in the case of ${}^6\text{He} + \alpha$. This confirms the validity of the three-body model, and the analysis is compatible with the conclusions of other authors of [10, 11].

REFERENCES

- [1] S. Sakuta *et al.*, *Phys. At. Nuclei* **72**, 1982 (2009).
- [2] T.A.D. Brown *et al.*, *Phys. Rev. C* **76**, 054605 (2007).
- [3] N. Burtebayev *et al.*, *Nucl. Phys. A* **909**, 20 (2013).
- [4] P. Descouvemont, D. Baye, *Phys. Lett. B* **505**, 71 (2001).
- [5] A. Tohsaki, H. Horiuchi, P. Schuck, G. Röpke, *Phys. Rev. Lett.* **87**, 192501 (2001).
- [6] M. Zhukov *et al.*, *Phys. Rep.* **231**, 151 (1993).

- [7] P. Navrátil, S. Quaglioni, I. Stetcu, B.R. Barrett, *J. Phys. G: Nucl. Part. Phys.* **36**, 083101 (2009).
- [8] C. Forssén, P. Navrátil, W. Ormand, E. Caurier, *Phys. Rev. C* **71**, 044312 (2005).
- [9] G. Ter-Akopian *et al.*, *Phys. Lett. B* **426**, 251 (1998).
- [10] Yu.T. Oganessian, V. Zagrebaev, J. Vaagen, *Phys. Rev. C* **60**, 044605 (1999).
- [11] D.T. Khoa, W. Von Oertzen, *Phys. Lett. B* **595**, 193 (2004).
- [12] G.R. Satchler, W.G. Love, *Phys. Rep.* **55**, 183 (1979).
- [13] Y. Suzuki, K. Varga, «Stochastic Variational Approach to Quantum-mechanical Few-body Problems, vol. 54», Springer Verlag, Berlin, Heidelberg 1998.
- [14] A. Antonov *et al.*, *Phys. Rev. C* **72**, 044307 (2005).
- [15] I.J. Thompson, *Comput. Phys. Rep.* **7**, 167 (1988).
- [16] N. Anantaraman, H. Toki, G. Bertsch, *Nucl. Phys. A* **398**, 269 (1983).
- [17] G. Satchler, «Direct Nuclear Reactions. International Series of Monographs on Physics, Vol. 68», Oxford University Press, 1983.
- [18] V. Avrigeanu, P. Hodgson, M. Avrigeanu, *Phys. Rev. C* **49**, 2136 (1994).